WAVES GENERATED BY A VERTICAL CYLINDER MOVING IN STILL WATER

J.R.CHAPLIN[1], R.C.T.RAINEY[2] & C H RETZLER[1]

[1] City University, London EC1; [2] WS Atkins Oil & Gas, London WC1

Abstract

To aid the understanding of the violent surface motions seen around fixed vertical cylinders in steep waves, experiments have begun at City University on a vertical cylinder moving in still water. Initial results, with sinusoidal cylinder motions, are presented here. Comparisons are made with linear predictions using an exact analytical solution. Various non-linear regimes are identified.

1. Introduction

Violent motion of the water surface is produced around a vertical cylinder by a long steep wave (e.g. length/diameter = length/height = 10, say, but without the wave breaking). A sheet of water is thrown up on the upwave side of the cylinder, which collapses to produce two small "edge waves" that run around the cylinder on each side, and run into each other on the downwave side. See Chaplin, Rainey & Yemm, 1997. The phenomenon is very poorly understood, and also of continuing importance to the offshore oil industry. On the UK continental shelf, for example, there has already been some serious structural damage to an offshore oil facility this winter, directly caused by such an event.

In a previous workshop paper (Rainey, 1997) it was argued that the same phenomenon may occur when a vertical cylinder suddenly changes its acceleration while moving in still water. This is because in that case violent surface motion is also predicted, by the small time expansion method. An interesting question is whether the two "edge waves" would also be seen – clearly if they are, many of the features of the original problem can be studied in this much simpler context.

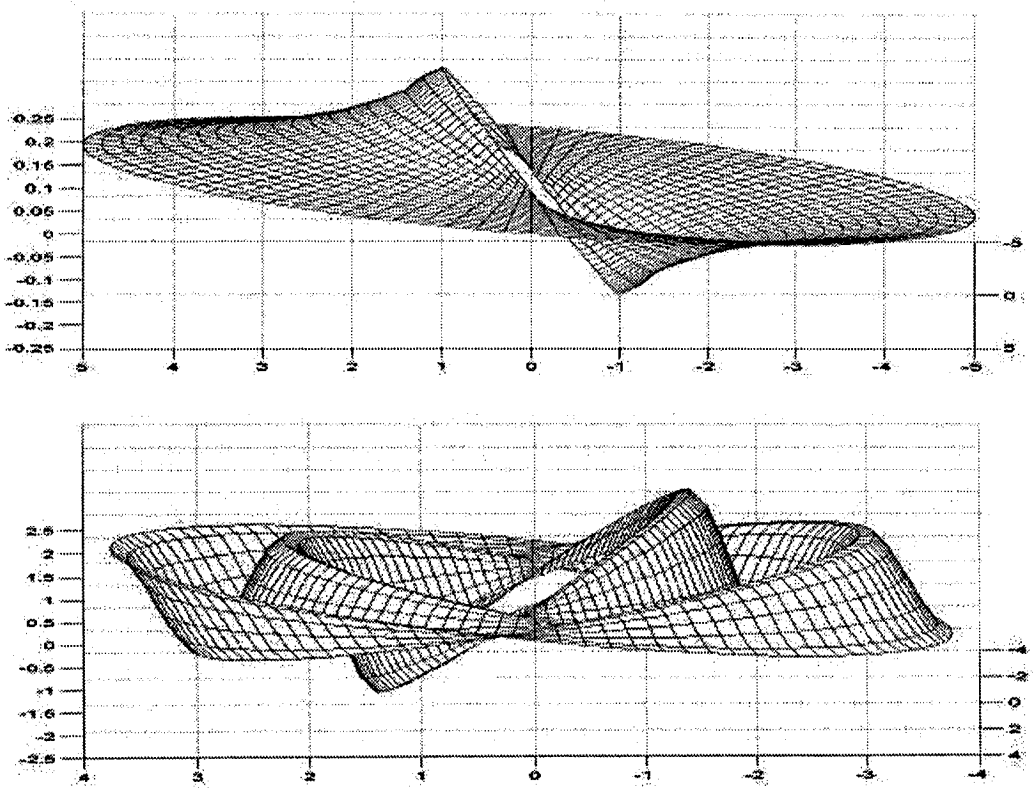

Figure 1. The free surface computed from linear theory for $k_0 = 0.2$ (in the upper diagram) and $k_0 = 4$ (in the lower diagram). In both cases the surface is shown at the instant at which the cylinder is moving with maximum velocity to the right.

2. Experimental arrangements

The experiments were carried out in a tank 2.4m square in plan, having a horizontal base and vertical sides, (all of glass) with a water depth of 0.5m. A servo-controlled carriage system, mounted 0.3m above the water surface, crosses the centre of the tank in a direction parallel to two of the sides. It carried the 200mm diameter vertical test cylinder, the horizontal base of which was a few millimetres above the floor of the tank. Waves radiated by the cylinder's motion were dissipated by an array of 30 vertical wedges of firm poly-ether foam which extended over the whole water depth. These were arranged in a circle, with their apexes pointing inwards at a radius of 0.65m from the centre of the tank.

In each experiment, the cylinder was oscillated for 10 cycles from rest at constant amplitude and frequency. Since the foam wedges were extremely efficient at dissipating the waves, all detectable movement of the surface had ceased well within 30s of the cylinder's being brought to rest. All measurements quickly achieved a steady state, and the results presented below were computed from data collected from the 4th to the 8th cycle. Two resistance-type wave gauges were mounted on the cylinder at a radial offset of 12mm from its surface, one on the axis of the motion ($\theta = 0$), and the other to the side ($\theta = \pi/2$).

3. Linear solution

A vertical cylinder moving in still water has, of course, a linear solution. Indeed, it has an exact analytical linear solution, which is conventionally given for sinusoidal motion as an infinite series, see Dean & Dalrymple, 1991, section 6.4. However, a much more elegant and numerically convenient form has recently been derived by McIver (1994). Taking length and velocity scales to be defined by the cylinder's radius and maximum velocity, in the usual cylindrical coordinates (r,θ,z, with z positive upwards and $\theta = 0$ the direction of the cylinder velocity $\Re\{e^{-i\omega t}\}$) the velocity potential ϕ is the real part of

$$\frac{-2\cos\theta}{\pi} e^{-i\omega t} \left\{ \int_0^\infty \frac{K_1(kr)\sin kz}{k^2 K_1'(k)}\, dk + \int_0^\infty \frac{C_1(kr)\, e^{kz}}{k(k-k_0)\,|H_1'(k)|^2}\, dk \right\}, \qquad (1)$$

where $C_1(kr) = J_1(kr)\,Y_1'(k) - Y_1(kr)\,J_1'(k)$, and for simplicity we are considering the infinite-depth case where $\omega^2 = gk_0$. The first integral is the solution for the boundary condition $\phi = 0$ on $z = 0$ and is simply derived, as described e.g. in Rainey (1997). It is readily evaluated with MATHCAD as shown there, and features a vertical velocity which approaches infinity as r approaches 1, thus giving the violent surface motion for transient motions, in the small-time expansion scheme, mentioned above.

The second integral converts the boundary condition on $z = 0$ to $\phi_z = \omega^2\phi$ and is much more complicated to derive. It is remarkably similar except that the path of integration must be taken beneath the singularity at $k = k_0$ in order to satisfy the radiation condition. Since the integrand is of the form $f(k)/(k - k_0)$, where $f(k)$ is analytic at $k = k_0$, the Laurent series of the integrand about $k = k_0$ has only one term with negative exponent, viz $f(k_0)/(k - k_0)$. Hence the small part of integral with its path beneath the real axis is simply $\pi i f(k_0)$. Thus this integral, too, can be readily evaluated with MATHCAD or MAPLE.

Total surface elevations (which can in fact be obtained from the second integral alone, via $i\omega\phi/g$, since in the first integral $\phi = 0$ on $z = 0$) are shown, for the cases $k = 0.2$ and 4 in figure 1. It remains finite, of course, as r approaches 1, so by implication the second integral has a singularity in the surface velocity, which cancels that in the first integral.

4. Experimental results

Measurements of the water surface elevation close to the cylinder at $\theta = 0$ for moderate amplitudes are in excellent agreement with linear theory, as shown in figure 2, where the normalised amplitude and phase of the fundamental frequency component of the motion are compared with analytical results. Normalised

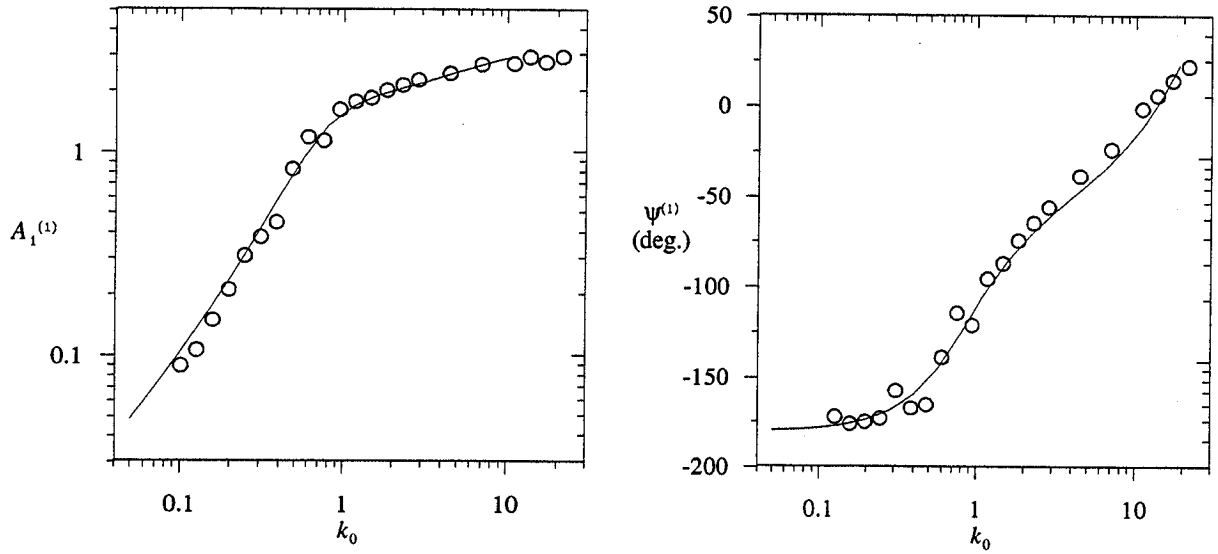

Figure 2. Amplitudes (on the left) and phases (on the right) of the water surface elevation adjacent to the cylinder's surface at $\theta = 0$. Lines are computed from the linear theory; measurements are shown as open circles.

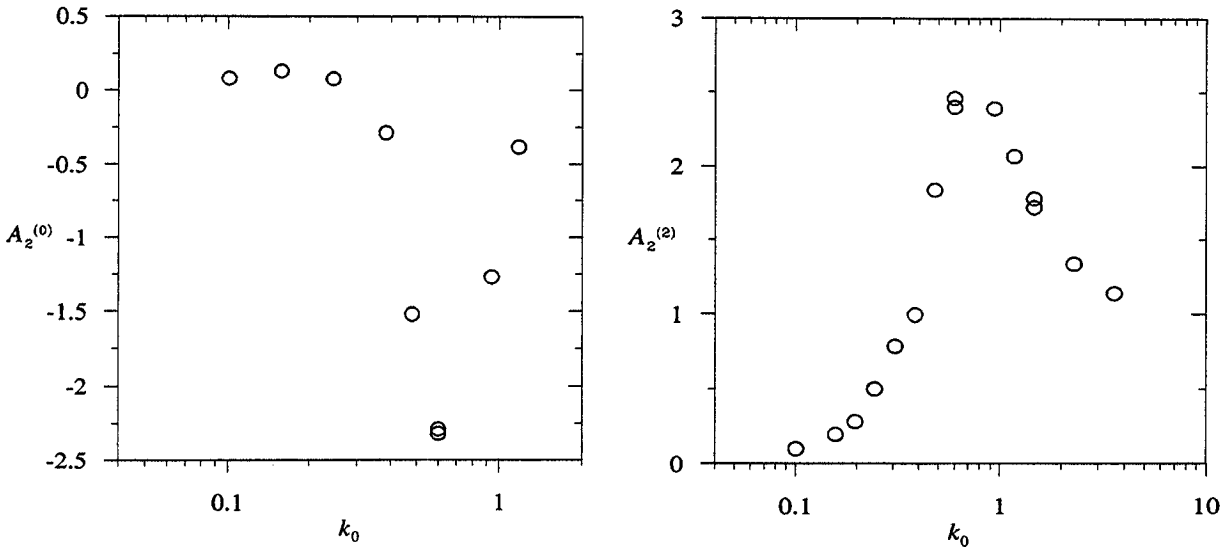

Figure 3. Non-linear features of the water surface elevation measurements adjacent to the cylinder at $\theta = \pi/2$. The diagram on the left shows the normalised mean water surface elevation, and that on the right the normalised amplitude of the oscillation at frequency 2ω.

amplitudes of water surface motion at frequency $m\omega$ are expressed throughout in the form $A_n^{(m)} X^n$, where X is the normalised amplitude of the cylinder's motion. It is noted that the large change in the phase of the water surface elevation with respect to that of the cylinder's motion is apparent also in figure 1. Slight discrepancies between measurement and theory at low k_0 may be associated with finite depth effects.

Since (1) has the factor $\cos\theta$, any surface elevation which does not vary as $\cos\theta$ must be non-linear. This applies in particular to any motion of the water surface on $\theta = \pi/2$, where measurements adjacent to the cylinder reveal components at zero frequency and at frequency 2ω. These are plotted in figure 3. The predominantly downward offset seen there, for example, is to be expected on second-order diffraction theory. A similar effect, caused by the Bernoulli pressure term, is exactly cancelled in undisturbed regular

waves by the effect of evaluating the surface pressure at the first-order wave elevation, rather than $z = 0$. But in the present case there is no such cancellation, because there is no first-order wave elevation.

Another non-linear feature of the measurements is the "edge wave" mentioned above. This is clearly evident at low values of k_0 (comparable with wavelength/diameter ration of 10 mentioned above) and is shown in the left hand photograph in figure 4. The frequencies of the tests shown in figure 4 match those of figure 1, and the phases are also approximately the same, though in the left hand image in figure 4, the cylinder has passed the point of maximum velocity.

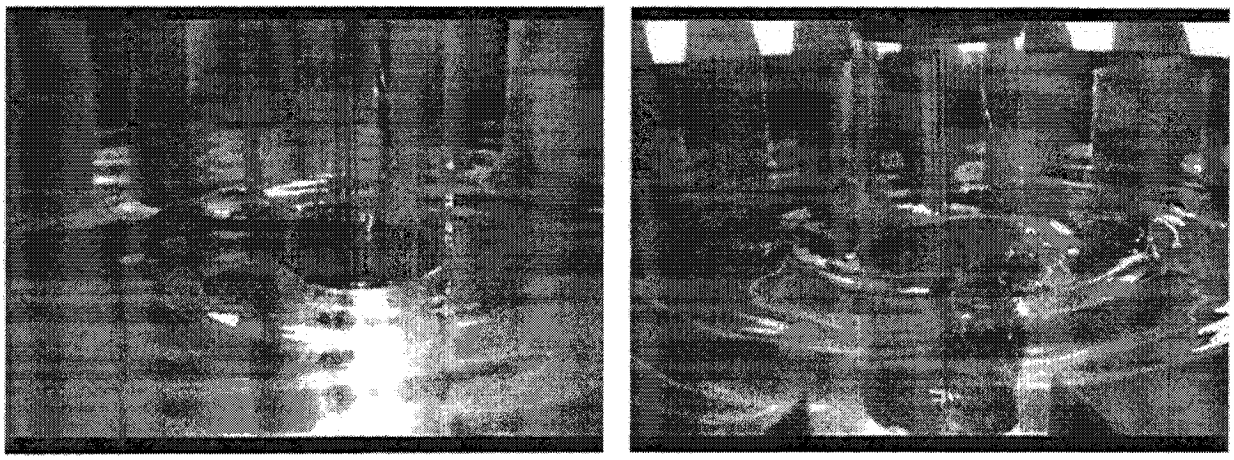

Figure 4. The free surface observed in the tank for $k_0 = 0.2$, $X = 0.43$ (on the left) and $k_0 = 4$, $X = 0.071$ (on the right). The wave absorbing poly-ether foam wedges can be seen in the background.

This work was supported by EPSRC (grant GR/L69879), with support in kind from WS Atkins plc.

References

Chaplin, J.R., Rainey, R.C.T. & Yemm, R.W. 1997 Ringing of a vertical cylinder in waves *J Fluid Mech.* 350, 119-147.

Dean,R.G. & Dalrymple, R.A. 1991 *Water Wave Mechanics for Engineers and Scientists* World Scientific

McIver, P.1994 Transient fluid motion due to the forced horizontal oscillations of a vertical cylinder *Applied Ocean Research* 16, 347-351

Rainey, R.C.T. 1997 Violent surface motion around vertical cylinders in large steep waves - is it the result of the step change in relative acceleration? *12th IWWWFB, Marseilles (ed. B.Molin)*